4D Automark: Change Point Detection and Image Segmentation for Time Series of Astrophysical Images

Cong Xu

With Hans Moritz Günther, Vinay L. Kashyap, Thomas C.M. Lee and Andreas Zezas

Department of Statistics
University of California, Davis

Feb 09, 2021

Outline

1. Background and Modeling
   - Problem Description
   - Modeling
   - Model Selection Using MDL
   - Theoretical Properties
2. Practical Algorithm
   - An Iterative Algorithm
   - Image Segmentation
   - Post-processing: Highlight Key Pixels
3. Application to Real Data
   - XMM-Newton Observations of Proxima Centauri
   - Isolated Evolving Solar Coronal Loop
4. Future Work

Outline

1. Background and Modeling
   - Problem Description
   - Modeling
   - Model Selection Using MDL
   - Theoretical Properties
2. Practical Algorithm
   - An Iterative Algorithm
   - Image Segmentation
   - Post-processing: Highlight Key Pixels
3. Application to Real Data
   - XMM-Newton Observations of Proxima Centauri
   - Isolated Evolving Solar Coronal Loop
4. Future Work

Problem Description

- Many phenomena in the high-energy universe are time-variable, from coronal flares on the smallest stars to accretion events in the most massive black holes.

Problem Description

- Many phenomena in the high-energy universe are time-variable, from coronal flares on the smallest stars to accretion events in the most massive black holes.

  Goal:

- Detect change points in the time direction (the times at which sudden changes happened during the underlying astrophysical process).
- Identify sources and locate their spatial boundaries.

Data

Data are usually obtained in the form of a list of photons.

- the two-dimensional spatial coordinates (x, y) where the photons were detected
- the times t they were recorded
- wavelengths w (i.e., energies)

Binning

- We first bin these data into a 4-D rectangular grid of boxes.
- A 4D table of photon counts indexed by the two-dimensional coordinates (x, y), time index t and energy band w.
- It can be viewed as a series of multi-band images with counts of photons as the values of the pixels.

Assumptions

- The emission times of photons can be considered a non-homogeneous Poisson process.
- The Poisson counts in each pixel are independent, and the image slices are also independent, since the grids do not overlap with each other.
- That is to say,

$$y_{i,t,w} \overset{i.i.d.}{\sim} \text{Poisson}(\lambda_{i,t,w}\Delta T_t),$$

Assumptions

- The underlying Poisson rate for each of the images follows a piecewise constant function.

A Model for Homogeneous Image Series

- A temporally homogeneous Poisson model without any change points.
- Each image can be treated as an independent Poisson realization of the same, unknown, true image.

A Model for Homogeneous Image Series

Piecewise Constant

- The 2-dimensional space of x-y coordinates is partitioned into m non-overlapping regions, such that all the pixels in a given region have the same Poisson intensity.

$$\lambda_{i,t,w} = \sum_{h=1}^{m} \mu_{h,w} I_{\{i \in R_h\}}.$$

- R_h: the index set of the pixels within the h^{th} region
- $\mu_{h,w}$: the Poisson rate for the w^{th} band of the h^{th} region.

Modeling with Change Points

Piecewise constant

- Suppose these images can be partitioned into $K+1$ homogeneous intervals by K change points

$$\tau = \{\tau_0 = 0,\ \tau_1, \tau_2, ..., \tau_K,\ \tau_{K+1} = N_{\mathrm{T}}\}$$

$$\lambda_{i,t,w} = \sum_{k=1}^{K+1} I_{\{t \in (\tau_{k-1}, \tau_k]\}} \sum_{h=1}^{m^{(k)}} \mu_{h,w}^{(k)} I_{\{i \in R_h^{(k)}\}},$$

Model Selection Using MDL

- Given the observed images $\{y_{i,t,w}\}$, we aim to obtain an estimate of $\lambda_{i,t,w}$.
- In other words, we want an estimate of the change points, the image partitions and the Poisson rates of the regions for each band.
- Estimating the partition is a complicated model selection problem.
- We will select the model by the minimum description length (MDL) principle.

Model Selection Using MDL

- The minimum description length (MDL) principle [Rissanen, 1989] defines the best model as the one that produces the best lossless compression (minimization of the code length) of the data.
- Code length: or description length, amount of hardware memory to store the thing

$$\text{MDL} = \text{CL}(\text{fitted model}) + \text{CL}(\text{data given fitted model})$$

  - First term: model complexity
  - Second term: data fidelity, negative of the conditional log-likelihood of data given fitted model

Model Selection Using MDL

- Why MDL?
  - It is computationally tractable for complex problems such as the one this paper considers.
  - It has been shown to enjoy excellent theoretical and empirical properties in other model selection tasks.

- Following the method in Lee [2000], the MDL criterion for segmenting N_{T} homogeneous images is

$$\mathrm{MDL}(m, R, \hat{\mu}) = m \log(N_{\mathrm{I}}) + \frac{\log(3)}{2} \sum_{h=1}^{m} b_h +$$

$$\frac{N_{\mathrm{W}}}{2} \sum_{h=1}^{m} \log(N_{\mathrm{T}} a_h) - \sum_{w=1}^{N_{\mathrm{W}}} \sum_{t=1}^{N_{\mathrm{T}}} \sum_{h=1}^{m} \sum_{i \in R_h} y_{i,t,w} \log(\hat{\mu}_{h,w}),$$

- The overall MDL criterion for the model with change points is

$$\begin{aligned} & \mathrm{MDL}_{\mathrm{overall}}(K, \tau, \mathcal{M}, \mathcal{R}, \hat{\boldsymbol{\mu}}) \\ = \quad & K \log(N_{\mathrm{T}}) + \sum_{k=1}^{K+1} \mathrm{MDL}(\tau_{k-1}, \tau_k, m^{(k)}, \boldsymbol{R}^{(k)}, \hat{\boldsymbol{\mu}}^{(k)}). \end{aligned}$$

- The best-fit model is defined as the minimizer of the criterion.

Consistency

The MDL-based model selection to choose the region partitioning, as well as the corresponding Poisson intensity parameters, is indeed strongly statistically consistent, under mild assumptions of maintaining the temporal variability structure of $\lambda_{i,t,w}$.

Outline

1. Background and Modeling
   - Problem Description
   - Modeling
   - Model Selection Using MDL
   - Theoretical Properties
2. Practical Algorithm
   - An Iterative Algorithm
   - Image Segmentation
   - Post-processing: Highlight Key Pixels
3. Application to Real Data
   - XMM-Newton Observations of Proxima Centauri
   - Isolated Evolving Solar Coronal Loop
4. Future Work

An Iterative Algorithm

Global minimization of $\mathrm{MDL}_{\mathrm{overall}}(K, \tau, \mathcal{M}, \mathcal{R}, \hat{\mu})$ is virtually infeasible when the number of images N_T and the number of pixels N_I are not small.

An Iterative Algorithm

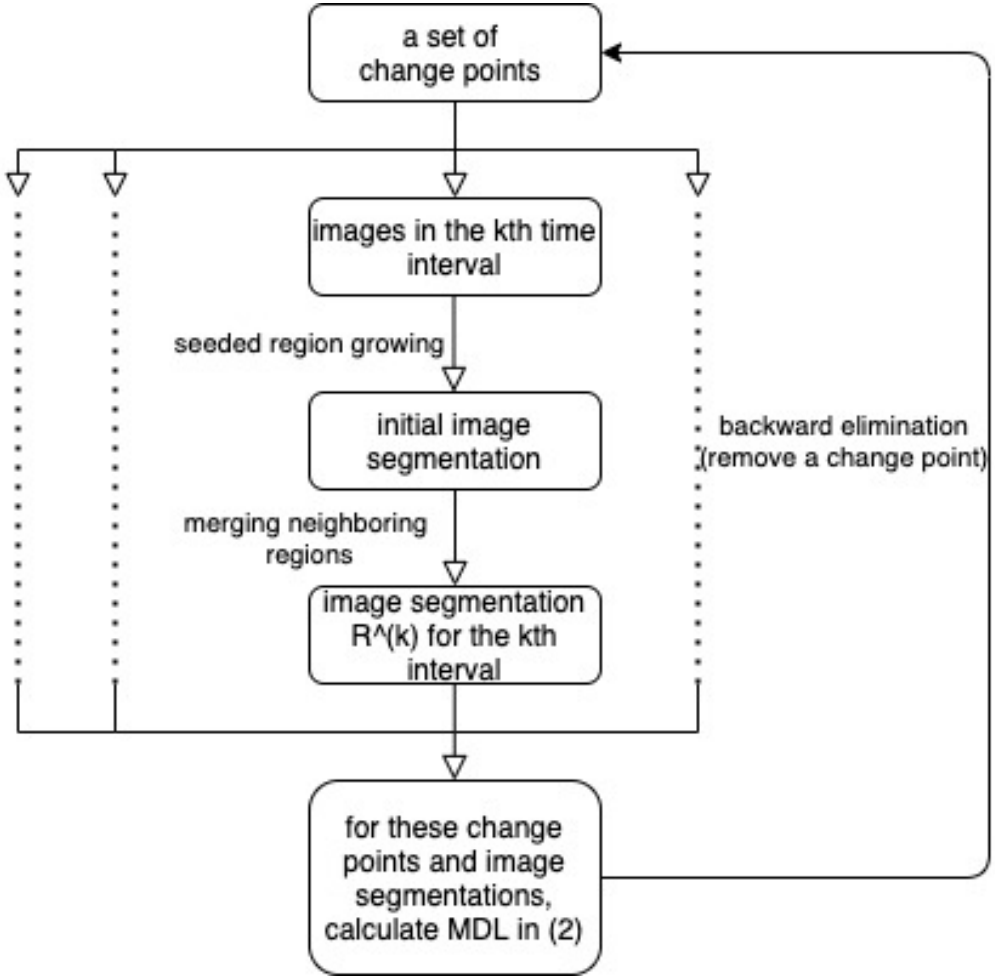

Figure: Schematic illustration of the minimization algorithm

An Iterative Algorithm

1. Given a set of change points, apply the image segmentation method to all the images belonging to the first homogeneous time interval and obtain the MDL best-fitting image for this interval. Repeat this for all remaining intervals. Calculate the MDL criterion.

2. Modify the set of change points by, for example, adding or removing one change point. In terms of what modification should be made, we use the greedy strategy to select the one that achieves the largest reduction of the overall MDL value.

Image Segmentation

Even for segmenting just one image, a global minimization of the MDL criterion is challenging.

Here we propose using the greedy region merging method to find the local minimizer of MDL.

- Finding an initial oversegmentation (a set of non-overlapping region segments)
- Region merging

Method: seeded region growing (SRG) by Adams and Bischof [1994]

- We select a set of seeds, manually or automatically, from the image. Each seed can be a single pixel or a set of connected pixels.
- A seed comprises an initial region.
- Then each region starts to grow outward until the whole image is covered.

Image segmentation

Initial oversegmentation

- At each step, the unlabelled pixels which are neighbors to at least one of the current regions comprise the set of candidates for growing the region.
- One of these candidates is selected to merge into the region, based on the Poisson likelihood that measures the similarity between a candidate pixel and the corresponding region.

We repeat this process until all the pixels are labeled, thus producing an initial segmentation by SRG.

Image Segmentation

Initial Oversegmentation

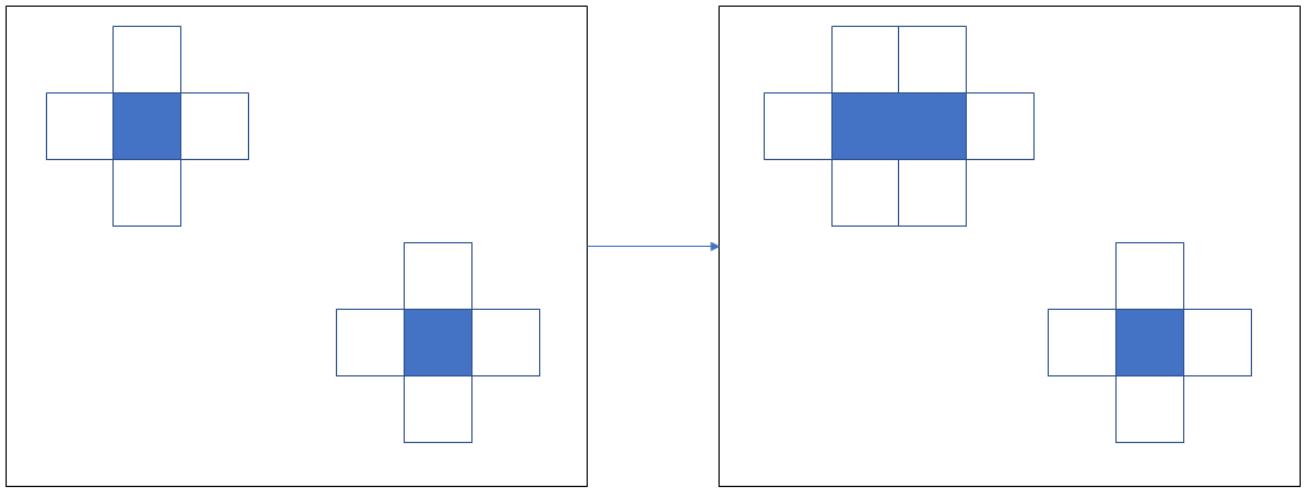

- Starting from the oversegmentation, at each step, we choose two neighboring regions and merge them into one region, such that the merging procedure provides the largest reduction (or the smallest increasing) in the MDL.
- The process continues until only one region left.
- Produce a sequence of nested segmentations and their MDL's
- Choose the segmentation with the smallest MDL.

Image Segmentation

Region Merging

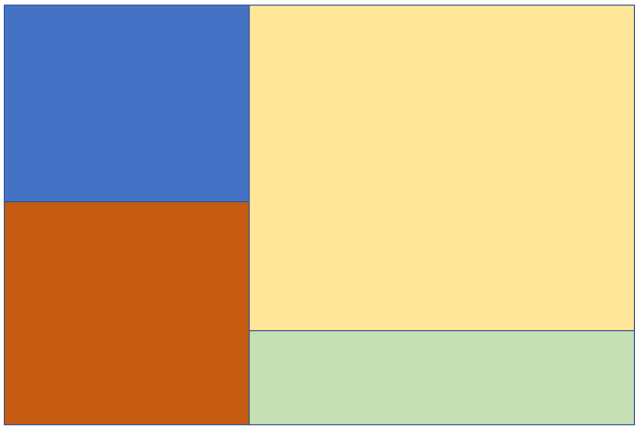

Image Segmentation

Region Merging

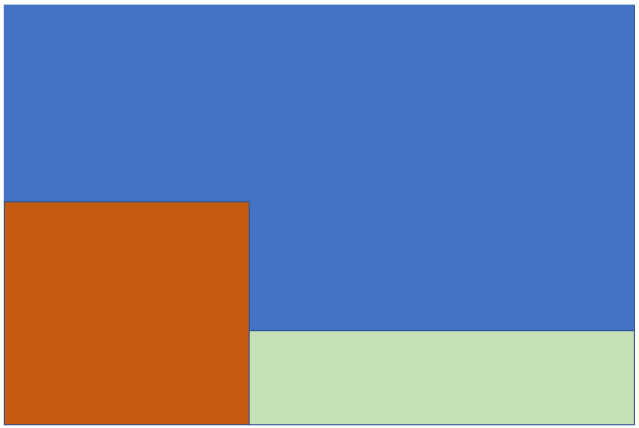

Image Segmentation

Region Merging

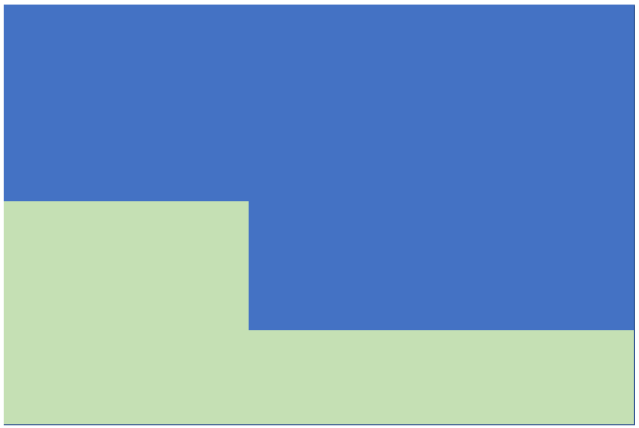

Highlight Key Pixels

- After the change points are located, it is necessary to locate the pixels or regions that contribute to the estimation of the change points.
- The manner by which such *key pixels* are identified depends on the scientific context.
- Below we present two methods.

Highlight Key Pixels

Based on Pixel Differences

- Define the difference d_i for pixel i as

$$d_i = \sqrt{\hat{\lambda}_i^{(k+1)}} - \sqrt{\hat{\lambda}_i^{(k)}} \,. \tag{1}$$

- A pixel is labelled as a key pixel if its d_i is far away from the mean of all the differences. To be specific, pixel i is labelled as a key pixel if

$$\left| \frac{d_i - \hat{\mu}}{\hat{\sigma}} \right| > \Phi^{-1}\left(1 - \frac{1}{2}p\right), \tag{2}$$

Highlight Key Pixels

Based on Region Differences

- Apply the square-root transformation to the pixels within each of the regions. Then we calculate the sample means $\hat{\mu}_1$ and $\hat{\mu}_2$ and sample variances $\hat{\sigma}_1^2$ and $\hat{\sigma}_2^2$ of these two groups of square-rooted values.
- Then we can for example test whether the difference between $\hat{\mu}_1$ and $\hat{\mu}_2$ is large enough with

$$\left| \frac{\hat{\mu}_2 - \hat{\mu}_1}{\sqrt{\hat{\sigma}_1^2 + \hat{\sigma}_2^2}} \right| > \Phi^{-1}\left(1 - \frac{1}{2}p\right). \tag{3}$$

Outline

1. Background and Modeling
   - Problem Description
   - Modeling
   - Model Selection Using MDL
   - Theoretical Properties
2. Practical Algorithm
   - An Iterative Algorithm
   - Image Segmentation
   - Post-processing: Highlight Key Pixels
3. Application to Real Data
   - XMM-Newton Observations of Proxima Centauri
   - Isolated Evolving Solar Coronal Loop
4. Future Work

Proxima Centauri

We use a dataset from XMM-Newton (Obs.ID 0049350101), where Proxima Centauri was observed for 67 ks on 2001-08-12 [Güdel et al., 2002].

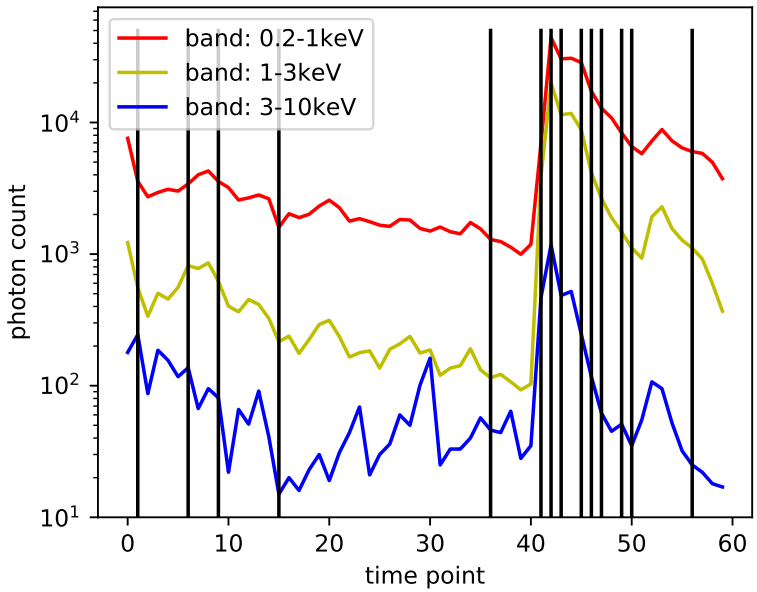

Figure: Light curves of Proxima Cen in different bands. Each curve denotes the number of photons within the corresponding band at a given time point index. Vertical black lines denote the locations of the detected change points.

Proxima Centauri

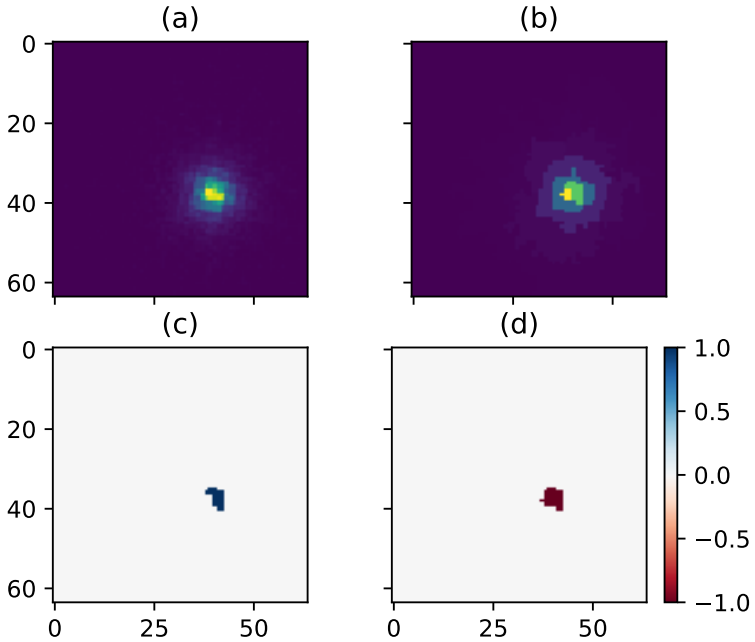

Figure: Results for Proxima Centauri. (a): the data image at time point 42 for the first band (200, 1000] in eV. (b): the corresponding fitted value $\lambda_{i,t,w}$. (c): regions that show an increase (blue) and decrease (red) in intensity prior to this time point. Compared with the previous time interval, there was a significant increase in the source at this time point. (d): as in panel *c*, but for the epoch after this time point. After this time point, the brightness in the source decreased. Notices that these two bottom plots share the colorbar, where the value 1 denotes increasing and -1 denotes decreasing intensities.

SDO/AIA

As a proof of concept, we apply the method to a simple case of an isolated coronal loop filling with plasma, as observed with the Solar Dynamics Observatory's Atmospheric Imaging Assembly (SDO/AIA) filters [Pesnell et al., 2012]

We consider AIA observations carried out on 2014-Dec-11 between 19:12 UT and 19:23 UT, and focus on a 64×64 pixel region located $(+1'', -271'')$ from disk center, in which a small, isolated, well-defined loop appeared at approximately 19:19 UT.

SDO/AIA

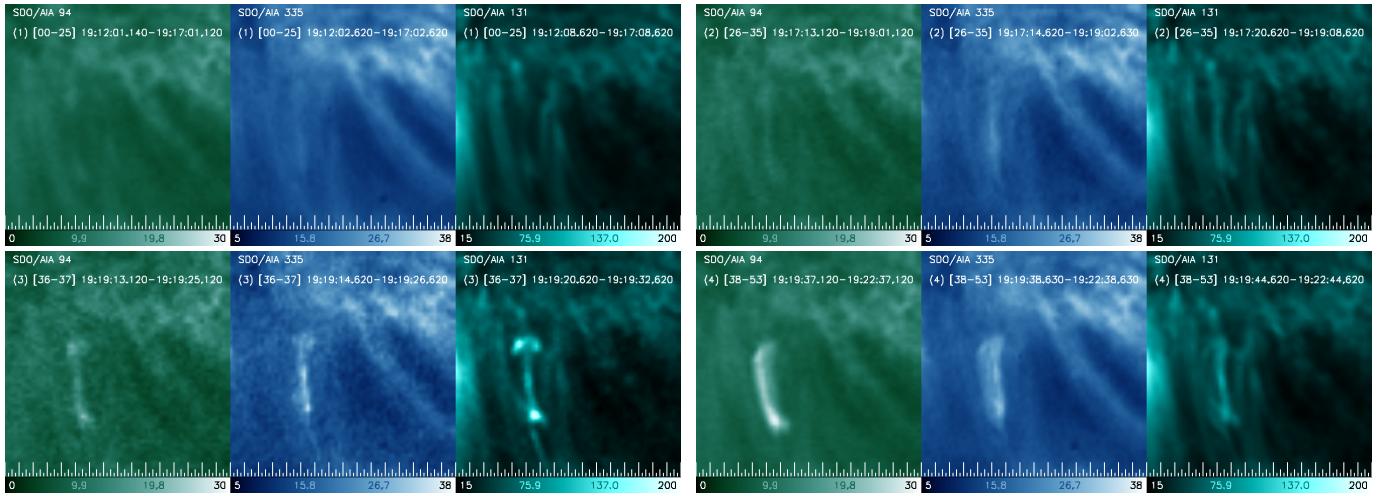

Figure: An isolated loop structure shown lighting up in 3 SDO/AIA passbands. Each row corresponds to the intensities in AIA filter images, averaged over the time duration found by our method, going from interval 1 (top left) to interval 4 (bottom right). The columns, going from left to right, show the 94, 335, and 131 Å filter band images.

SDO/AIA

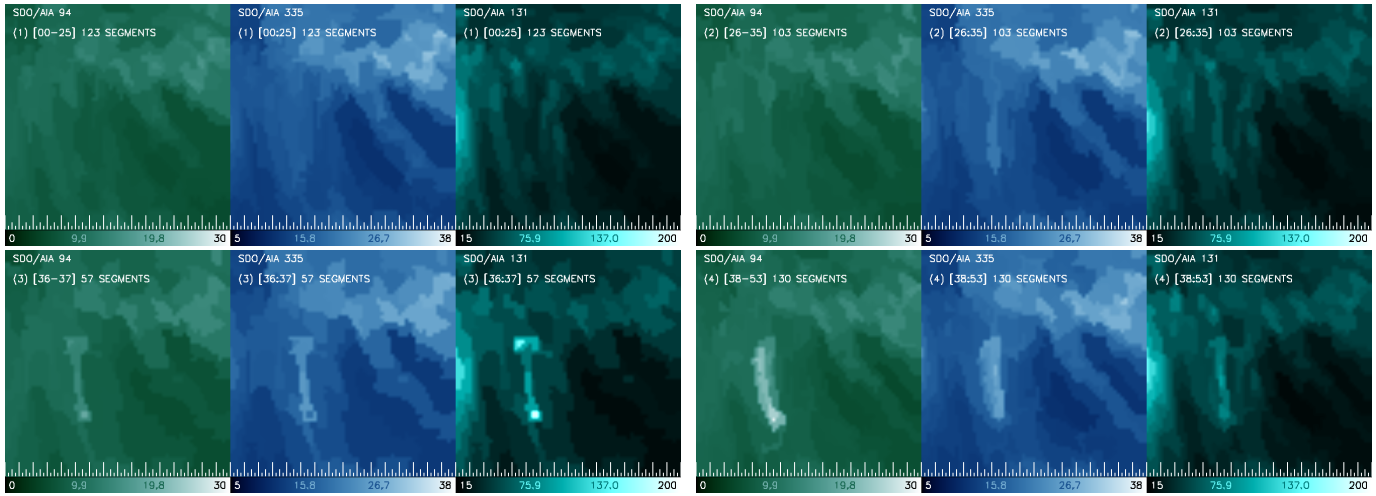

Figure: Intensities $\lambda_{i,t,w}$ as fit to the data. The images are arranged in the same manner, and demonstrate that the loop structure is locatable and identifiable. The number of region segments found are also marked.

SDO/AIA

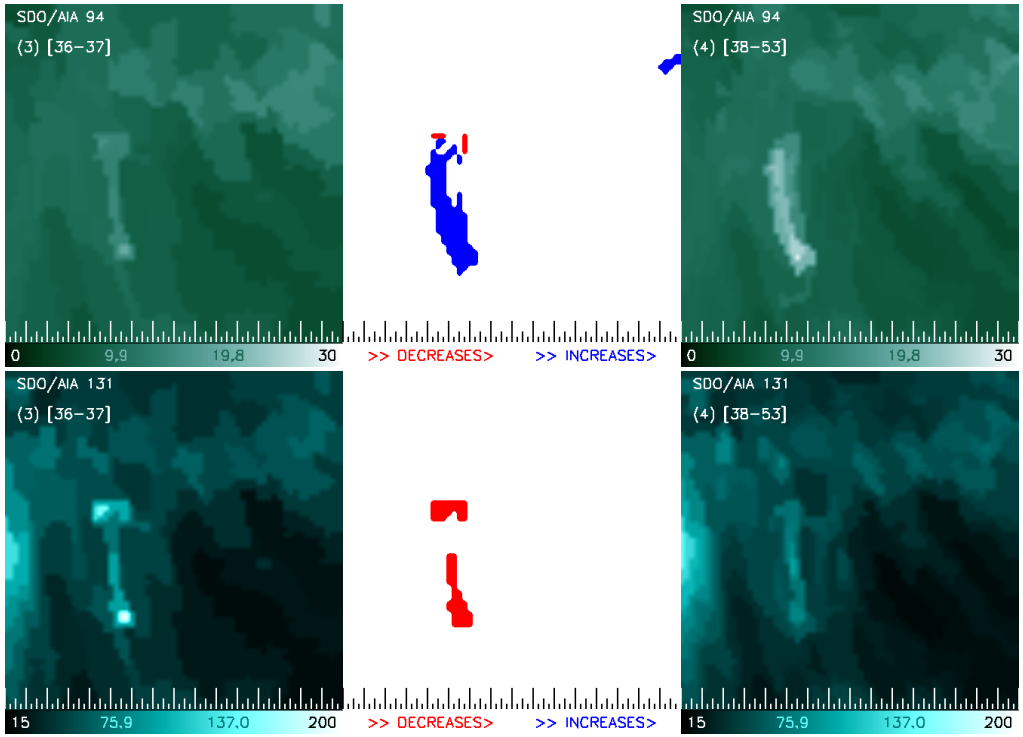

Figure: Demonstrating the isolation of key pixels of interest. Each set of three shows the fitted intensity in one passband in the 3rd interval (*left*), followed by a bitmap of pixels (*middle*) showing where intensity increases (blue) and decreases (red), followed by the fitted intensity image in the same filter in the 4th time interval (*right*). The upper row shows the transition in the 94 Å filter, and the lower row shows the transition in the 131 Å filter. Notice that the loop continues to brighten at 94 Å, even as it starts to fade at 131 Å.

SDO/AIA

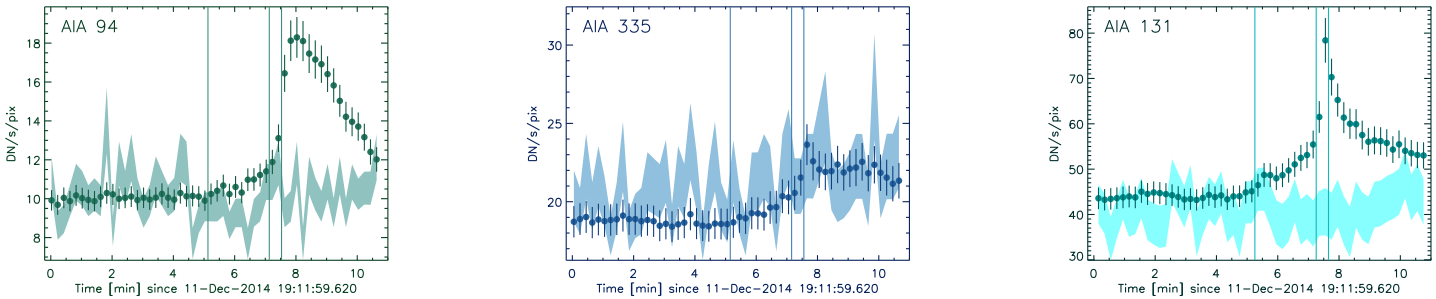

Figure: Light curves of the key pixels where changes are found, for the three filters used in the analysis: 94 Å (*left*), 335 Å (*middle*), and 131 Å (*right*). The average of the observed intensities, weighted by the number of times each pixel is flagged as a key pixel, are shown as dots, along with the similarly weighted sample standard deviation as vertical bars. The shaded regions represent the envelope of the sample standard deviation seen *outside* the flagged pixels. The vertical lines denote the change points found by our algorithm.

Outline

1. Background and Modeling
   - Problem Description
   - Modeling
   - Model Selection Using MDL
   - Theoretical Properties
2. Practical Algorithm
   - An Iterative Algorithm
   - Image Segmentation
   - Post-processing: Highlight Key Pixels
3. Application to Real Data
   - XMM-Newton Observations of Proxima Centauri
   - Isolated Evolving Solar Coronal Loop
4. Future Work

Future work

- It will be helpful to quantify the evidence of the existence of a change point by deriving a test statistic based on Monte Carlo simulations or other methods.
- Another possible extension is to relax the piecewise constant assumption and allow piecewise linear/quadratic modeling so that the method is able to capture more complicated and realistic patterns.

References

Rolf Adams and Leanne Bischof. Seeded region growing. *IEEE Transactions on Pattern Analysis and Machine Intelligence*, pages 641–647, 1994.

Manuel Güdel, Marc Audard, Stephen L. Skinner, and Matthias I. Horvath. X-Ray Evidence for Flare Density Variations and Continual Chromospheric Evaporation in Proxima Centauri. *The Astrophysical Journal*, 580(1):L73–L76, Nov 2002. doi: 10.1086/345404.

Thomas C. M. Lee. A minimum description length-based image segmentation procedure, and its comparison with a cross-validation-based segmentation procedure. *Journal of the American Statistical Association*, pages 259–270, 2000.

W. Dean Pesnell, B. J. Thompson, and P. C. Chamberlin. The Solar Dynamics Observatory (SDO). , 275(1-2):3–15, January 2012. doi: 10.1007/s11207-011-9841-3.

Jorma Rissanen. *Stochastic Complexity in Statistical Inquiry Theory*. World Scientific Publishing Co., Inc., USA, 1989. ISBN 9971508591.